11th International Conference on Vibration Problems
Z. Dimitrovová *et al.* (eds.)
Lisbon, Portugal, 9-12 September 2013

DYNAMIC BEHAVIOUR OF A STEEL FOOTBRIDGE UNDER PEDESTRIAN LOADS

Loris Vincenzi[1], Elisa Bassoli*[1], Paola Gambarelli[1]

[1]DIEF – University of Modena and Reggio Emilia
{loris.vincenzi, elisa.bassoli, paola.gambarelli}@unimore.it

Keywords: steel footbridge, experimental tests, dynamic identification, pedestrian dynamic loads.

Abstract. *Footbridges are generally effective structures concerning the static behavior, since they are subjected to a limited level of live loads. Nevertheless, the frequency range of the pedestrian dynamic actions may fall within the natural frequency interval of the structure, giving high dynamic amplifications. Therefore, dynamic properties of footbridges and effects of pedestrian loads need to be analyzed, comparing experimental and numerical results.*
This paper is part of a research that aims to characterize the dynamic behavior of a steel footbridge with reference to pedestrian dynamic amplifications. The structure, located in Reggio Emilia (Italy), is about 170 meters long and composed of 5 simple-supported spans, linked at lower-floor level. To investigate the dynamic behavior of the footbridge, an experimental campaign has been first performed. Accelerations due to ambient vibrations (wind) and to pedestrian dynamic actions were recorded. In particular, a wide number of pedestrian dynamic loading conditions have been considered, such as excitations induced by people jumping, running and walking with different passing frequencies. Accelerations were acquired by an advanced MEMS-based system. 10 biaxial MEMS sensors were arranged in 3 different setups in order to identify as many natural modes as possible and to investigate the vibration level in several components of the footbridge.
The post-processing of experimental data allows to determine both the dynamic properties of the structure (frequencies, mode shapes and damping ratios) and the maximum accelerations caused by pedestrian actions. The dynamic characteristics are identified by means of the classic Enhanced Frequency Domain Decomposition (EFDD) method that is based on the diagonalization of the spectral density matrix.
Then, a finite element model is built and calibrated such that the analytical dynamic predictions agree with the experimental modal properties. Finally, the measured accelerations caused by pedestrian dynamic actions are compared with those given by the numerical model, considering different dynamic load models.

1 INTRODUCTION

Footbridges are very slender structures; their design is often governed by their serviceability behaviour, mainly concerning the fulfilment of the pedestrian comfort criteria. The slenderness of the structural solutions and the use of deformable elements and materials run counter to the satisfaction of the serviceability restrictions. Over the last decades, several experiences of high vibration level caused by pedestrian-induced loading have been reported [1-2]. Nowadays, the pedestrian-bridge interaction phenomenon has to be taken into account in footbridge design and excessive vibrations has to be avoided. In Building codes, this dynamic problem is considered by giving limits for the structural natural frequencies. Otherwise, if the natural frequencies fall within the excitation range, dynamic analyses must be performed considering adequate and reliable pedestrian loading models. The obtained accelerations have to be acceptable according to comfort criteria. Despite the increasing scientific interests and the international guideline recommendations, footbridges still remain prone to high levels of vibration; in many cases, problems may likely arise due to lateral vibrations, which people are much more sensitive to. Reliability of numerical results strongly depends on hypothesis introduced, usually provided in terms of constrains, masses, mechanical proprieties, etc. Correspondence between theoretical data, used in computation, and real parameters of structures must then be verified especially dealing with those characterizing the structural dynamic behaviour.

In this paper, the dynamic behaviour under pedestrian dynamic actions of the Correggio footbridge is investigated. An experimental campaign has been first performed. Accelerations due to ambient vibrations (wind) and to pedestrian dynamic actions were recorded, considering a wide number of pedestrian dynamic loading conditions. Pedestrian loading models are evaluated and dynamic analyses of the footbridge under pedestrian actions are performed. To obtain reliable results, a finite element model of the footbridge is first calibrated with respect to experimental modal parameters. The footbridge dynamic characteristics are obtained with an identification process by means of the classical Enhanced Frequency Domain Decomposition (EFDD) method.

2 THE CORREGGIO FOOTBRIDGE

The Correggio steel footbridge (Figure 1*a*) was built in 2011 in Reggio Emilia (Italy). It is 168 m long and it is composed of 5 simple-supported spans, linked at lower-floor level. The central span is 40 m long while the laterals are 32 m long each one. The footbridge is supported by 4 piles; the central and lateral piles are about 5.20 m and 2.80 m high respectively.

(*a*) (*b*)

Figure 1: The Correggio footbridge

The structure has a box cross-section 3.00 m x 2.85 m composed of truss girders (Figure 1*b*). Piles and trusses are made up by rectangular hollow profiles and L-shaped profiles are used for the lower lateral bracing system. The deck is 3 m wide and consists of a wooden plank resting on a corrugated sheet. The whole structure is slender, lightweight and characterized by sensitive vibrations due to pedestrian, cyclist and wind effects. Preliminary numerical studies indicated that the first (lateral) mode may be critical, due to the proximity to the frequency of lateral excitation induced by pedestrians. For this reason, a dynamic campaign and numerical dynamic analyses are performed to verify the respect of serviceability conditions.

3 DYNAMIC IDENTIFICATION

To characterize the footbridge dynamic behaviour, experimental dynamic tests have been performed. The modal properties of the structure have been identified by applying identification techniques to the measured data. The acquisition system and the experimental tests are described in the following subsections, while the identification algorithm and the results are reported in subsections 3.3 and 3.4.

3.1 The acquisition system

The dynamic tests have been performed by means of the SHM602 system [3]; it is an advanced integrated system for Structural Health Monitoring that relies on digital technologies, developed by Teleco and designed in collaboration with the Bologna University. It is composed of a storage/controller unit and MEMS-based sensing units connected to the controller via a serial bus. The sensor bus connection assures a high degree of reliability and prevention against electromagnetic interferences. Each sensing unit can record accelerations along two orthogonal axes and the temperature. All the acquired information is sent to the main unit with a sampling frequency that can be chosen by users. The sensing units are also able to perform the identification of local dynamic models in the time domain.

3.2 The dynamic tests

Aims of dynamic tests are to evaluate both the modal properties of the footbridge and the effect of pedestrian dynamic actions, recording accelerations caused by ambient vibrations (in operational conditions) and by people walking, running and jumping.

To estimate as many natural modes as possible, the footbridge dynamic behaviour was monitored using 10 sensors that were arranged in 3 different setups. Since each sensor can record the accelerations along two orthogonal axes, 20 measurement channels for each setup (10 in the vertical and 10 in the transverse direction) were available. Positions of sensors in

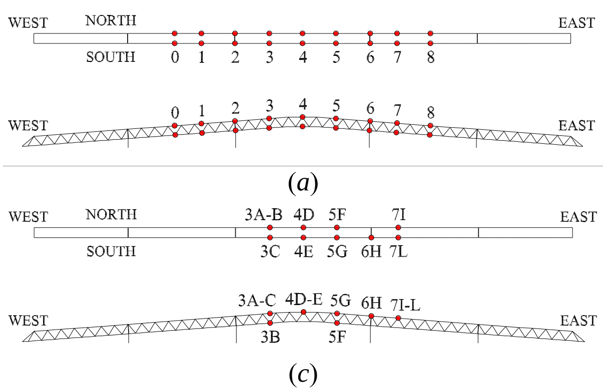

Figure 2: (*a*) Position numbering and (*b*-*d*) the 3 experimental setups.

the different setups are shown in Figure 2, where the letter denotes the sensor and the number represents the global position. In the first two setups, sensors were mainly located in the central span, placed on both the upper and lower chord of the main truss girders and on both deck sides (north side and south side in Figure 2) to evaluate the relative lateral displacement of the cross-section and to identify also torsional mode shapes. In the third configuration, the sensors were all positioned at the upper chord level of the south side, to cover the maximum possible length of the footbridge. In the latter setup, sensors were located at midspan, at quarters and close to the piles of the three central spans. To combine results obtained from the three setups, some sensors were kept at the same locations.

Results show that vertical accelerations are about 5-6 mg (where accelerations are given with respect to the gravity acceleration g) in the walking. In Figure 3, vertical and lateral accelerations induced by people running and jumping are reported. Values of about 40-60 mg (400-600 mm/s^2) are caused by two people running, whereas the lateral acceleration has values between ± 30 mg. Effects of about 20 seconds of jumping and of one single jump are shown in Figure 3*c*,*d*. Vertical and horizontal accelerations reach values of about 100 mg and 20 mg, respectively. Note that after each jump, the vertical acceleration damps in a few seconds while not negligible accelerations are measured also 50 seconds after as for the horizontal vibrations are concerned.

3.3 Identification algorithm

To identify the footbridge dynamic parameters, the Power Spectral Density (PSD) [4] matrix of the acquired accelerations ($\mathbf{G}_{yy}$) is calculated. Due to the hypothesis of (unknown) white noise load and lightly damped model, the PSD matrix can be expressed depending on the system dynamical properties, i.e.:

$$\mathbf{G}_{yy}(f) = \mathbf{H}(f)\mathbf{G}_{xx}(f)\mathbf{H}(f)^H = \sum_{k \in Sub(f)}^{N} \frac{d_k \boldsymbol{\varphi}_k \boldsymbol{\varphi}_k^T}{if - \lambda_k} + \frac{d_k \boldsymbol{\varphi}_k \boldsymbol{\varphi}_k^H}{if - \bar{\lambda}_k} \tag{1}$$

where φ_k is the k-th mode shape and d_k is a scaling factor. In case of resonance (corresponding to a peak of the PSD graph) the k-th mode contribution to the motion prevails and the Eq. (1)

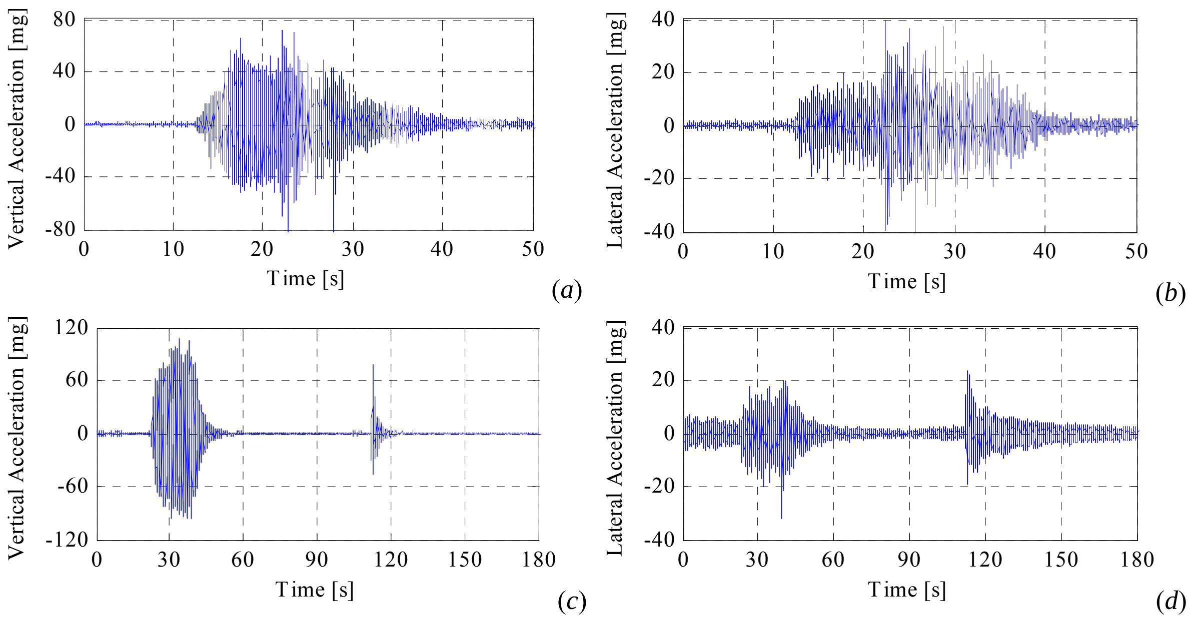

Figure 3: Vertical (*a*) and lateral (*b*) accelerations due to running recorded by the sensors 7L (setup 3); vertical (*c*) and lateral (*d*) accelerations due to jumping recorded by the sensors 5F (setup 1)

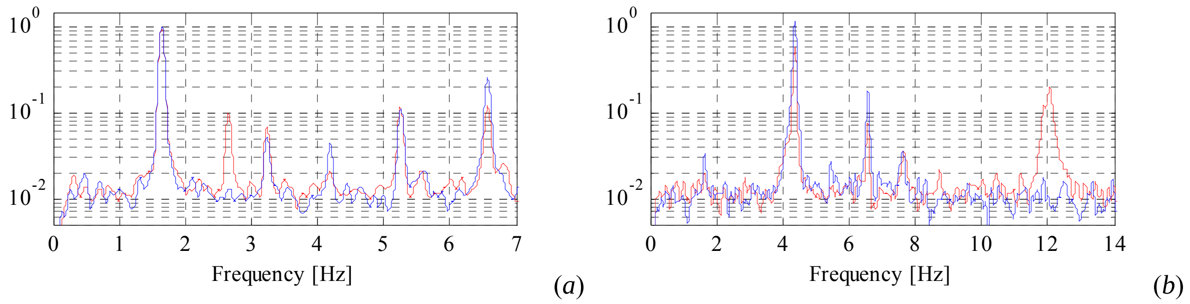

Figure 4: PSDs obtained from the lateral (*a*) and vertical (*b*) accelerations recorded by the sensors 5G and 4E in the first setup

becomes:

$$\mathbf{G}_{yy}(f)_{f \to f_k} = d_k \boldsymbol{\varphi}_k \boldsymbol{\varphi}_k^{\ H} \tag{2}$$

Further, the EFDD method relies on a singular value decomposition of the PSD matrix:

$$\mathbf{G}_{yy}(f_z) = \mathbf{U}_i \mathbf{S}_i \mathbf{U}_i^{\ H} \tag{3}$$

where $\mathbf{S}_i$ is a diagonal matrix that contains the singular values s_i and $\mathbf{U}_i$ is a matrix whose elements are the corresponding singular vectors $\mathbf{u}_i$. When the *k*-th mode contribution prevails (resonance) the Eq. (3) becomes:

$$\mathbf{G}_{yy}(f_z)_{f_z \to f_k} = s_{z,1} \mathbf{u}_{z,1} \mathbf{u}_{z,1}^{\ H} \tag{4}$$

Comparing the Eqs. (2) and (4), it is deduced that the singular vector represents the *k*-th mode shape while the singular value is the amplification factor, which represents the structure response amplification under dynamic loads. For each natural mode, the frequency corresponds to the peak of the PSD graph. After, the PSD is decomposed into single degree of freedom systems and the damping ratio is calculated through the logarithmic decrement. For all details about the method see [5].

3.4 Experimental results

The procedure previously described is applied to the measured data. Examples of PSD functions obtained from vertical and horizontal (transverse) accelerations are reported in Figure 4. Through the PSDs, the decomposed function is calculated and the results hereinafter reported are obtained. Natural frequency, mode shape and damping ratio are identified for each natural mode. A total of 10 modes (6 lateral modes, 2 verticals and 2 torsionals) with frequencies in the range 1.67 ÷ 12.08 Hz are clearly identified. Frequencies of identified modes are reported in Table 1, as well as a comparison with those obtained from the finite element model of the footbridge (see the next section). Moreover, four representative modes are shown in Figure 5. The blue and the green lines represent the upper chord level of the south side and of the north side respectively, while the red one represents the lower chord level of the north side. The first four modes show deformations mainly involved in the horizontal direction; moreover, the first vertical mode (mode no. 5) has frequency almost 2.5 times the first lateral, thus confirming the high flexibility of the footbridge in the horizontal direction.

4 DYNAMIC ANALYSES

First, a finite element model is built and calibrated. Truss and beam elements are used for

Mode No.	Mode Type	Experimental Frequency [Hz]	Damping Ratio [%]	Numerical Frequency [Hz]	Error [%]	MAC [%]
1	1st Lateral	1.674	0.82	1.676	+0.12	99.04
2	2nd Lateral	2.663	0.61	2.702	+1.46	98.43
3	3rd Lateral	3.082	0.45	3.103	+0.68	83.72
4	4th Lateral	3.567	0.67	3.489	-2.19	93.24
5	1st Vertical	4.392	0.98	4.293	-2.25	96.62
6	Lateral - central span	5.276	0.76	5.236	-0.76	86.39
7	Lateral - side spans	5.970	0.53	6.096	+2.11	65.78
8	1st Torsional	6.596	0.59	6.521	-1.14	85.87
9	Torsional - central span	7.690	0.80	7.918	+2.96	85.61
10	2nd Vertical	12.085	0.32	11.063	-8.46	96.68

Table 1: Experimental and numerical modes

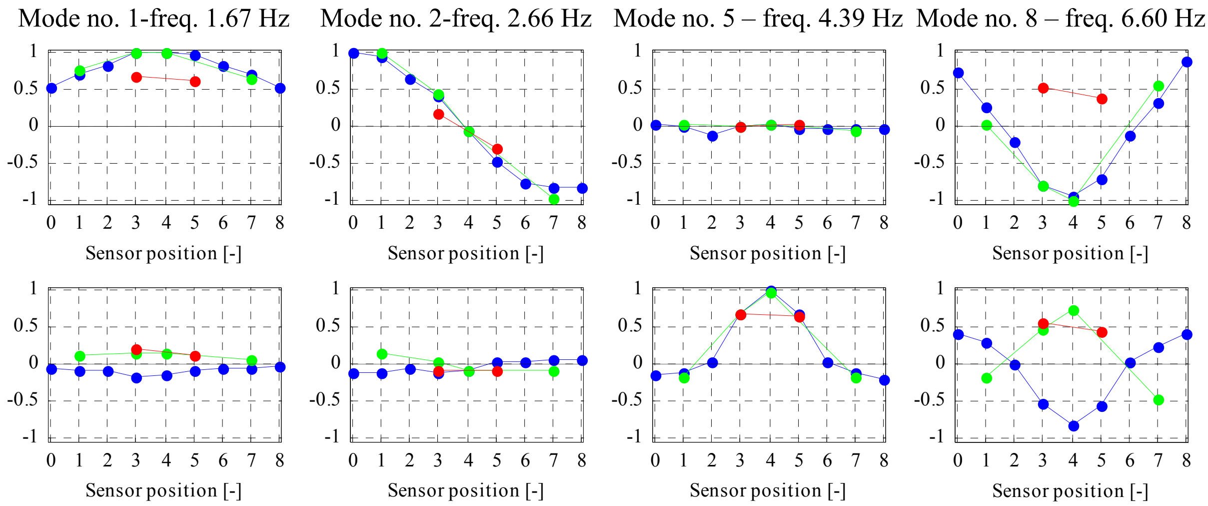

Figure 5: Lateral (first row) and vertical (second row) components of the mode shapes

girders and piles; constraints are applied at the base of piles and at the lateral span ends.

An updating procedure is performed to calibrate the model, so that the numerical results correspond as closely as possible to the experimental ones. For this purpose, a set of (unknown) model parameters are adjusted such that frequencies of modes no. 1, 2, 5 and 8 match the experimental ones. To obtain a reliable comparison, the numerical and the experimental mode shapes are first coupled by using the MAC [6]. The selected model parameters are the mass of the members (to take into account additional masses of plates and bolds) and the mass of the deck. In Table 1 the numerical frequencies obtained after the model calibration are compared with those identified experimentally. The values of the MAC are also reported. Numerical results match accurately the experimental ones with error never greater than 3% as for the first 9 frequencies and about 8% for the tenth. MAC values are also good, except for the 7-th mode, where the MAC value is only the 65%. This poor correlation is due to some disagreements in the horizontal components of the central span: experimental values are close to zero while not negligible values are obtained in the numerical model.

After the model was calibrated, dynamic analyses have been carried out to reproduce pedestrian dynamic loads and, consequently, to compare experimental and numerical maximum accelerations. To perform dynamic analyses, a mathematical model representing the dynamic forces due to a single pedestrian or a crowd of people crossing the structure is needed. The adopted model is described in the next subsection.

4.1 Pedestrian dynamic loads

During walking on a structure, pedestrians induce dynamic forces that have components in all three directions. Several studies [7-11] were performed to characterize the loads produced by pedestrians on structures. Most of these studies show that the induced forces depend on the pacing frequency, the walking (or running) speed and the step length. Defining f_p the pacing frequency, with time step length $T_p = 1/f_p$, the walking speed v can be approximately related to the pacing frequency [12]:

$$v = 0.9 f_p \tag{5}$$

It follows that the higher the walking speed is, the greater the pacing frequency becomes, whereas the step length decreases. Typical vertical forcing frequencies due to walking, running and jumping for both vertical and horizontal direction [8-10] and the corresponding pedestrian velocity are reported in Table 2.

To estimate the pedestrian-induced forces, the most widely used model is a periodic load model, based on the approximation of the single pedestrian load in a Fourier series. Considering the pedestrian action periodic and constant in time, the vertical force $F_v(t)$ induced by a person crossing the footbridge can be decomposed into a static part corresponding to the weight of the pedestrian Q and a dynamic part. The dynamic part can be expressed as a Fourier series with frequencies an integer multiple of the pacing frequency f_p:

$$F_v(t) = Q(1 + \sum_{k=1}^{n} \alpha_{n,v} \sin(2\pi n\, f_p t + \varphi_{n,v})) \tag{6}$$

To take into account the effect of pedestrian groups, the load induced by a single pedestrian Q has to be increased considering the pedestrian number n. In [7,9] an amplification factor equal to n in the case of pedestrian synchronization or $\sqrt{n}$ otherwise is suggested. The horizontal force $F_h(t)$ is defined considering only the dynamic component. According to several experimental evidences, the horizontal forcing frequency is reduced by a factor of 2 with respect to the vertical one, obtaining:

$$F_h(t) = Q \sum_{k=1}^{n} \alpha_{n,h} \sin(2\pi n (f_p/2)\, t + \varphi_{n,h}) \tag{7}$$

Terms $\alpha_{n,v}$, $\alpha_{n,h}$ are the Fourier's coefficients of the n-th harmonic, i.e. the dynamic load factor, in the vertical and horizontal direction respectively, while $\varphi_{n,v}$ and $\varphi_{n,h}$ represent the phase angles (timely phase shift) of the upper harmonics with respect to the 1st harmonic. Coefficients $\alpha_{n,v}$, $\alpha_{n,h}$ depend on the pedestrian velocity; the increasing walking speed lead to higher peak force magnitude and, so, the values of $\alpha_{n,v}$ and $\alpha_{n,h}$. Several measurements and studies have been performed to quantify the values of $\alpha_{n,v}$, $\alpha_{n,h}$, $\varphi_{n,v}$ and $\varphi_{n,h}$, some of which results are reported in [7-10,12]. Typical values for the first harmonic are reported in Table 2.

According to [8-9], in this work the first three harmonics are assumed to be adequate to represent the vertical pedestrian action, while four harmonics are needed to represent the transverse one. The dynamic load factors and the phase angles adopted to estimate the vertical and transverse pedestrian actions are reported in Table 3.

Dynamic analyses are performed considering the horizontal and vertical forces due to a single step applied to consecutive nodes of the footbridge model, to simulate the pedestrian walking. For each node, forces are defined by the Eqs. (6), (7) for values of time t between t_i and $t_i + T_p$ and equal to zero otherwise. Typical shapes of one single step force and of continuous walking forces are shown in Figures 6, 7 for the vertical and lateral direction, respectively. The blue and the red line represent forces associated to the right and the left foot.

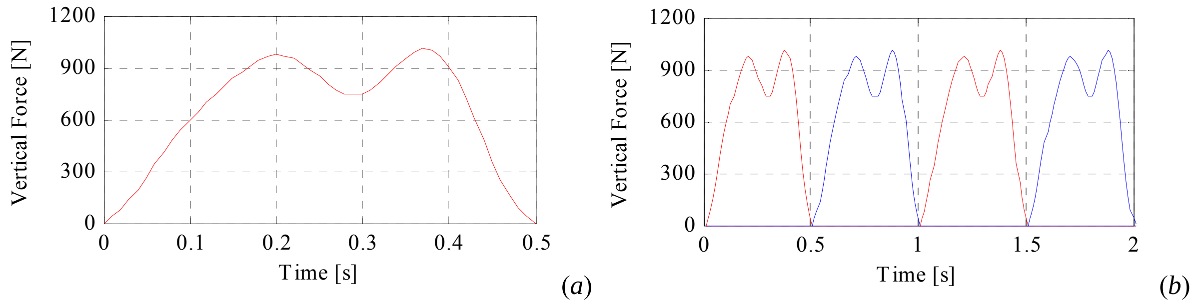

Figure 6: One step (*a*) and periodic walking (*b*) time histories in vertical direction

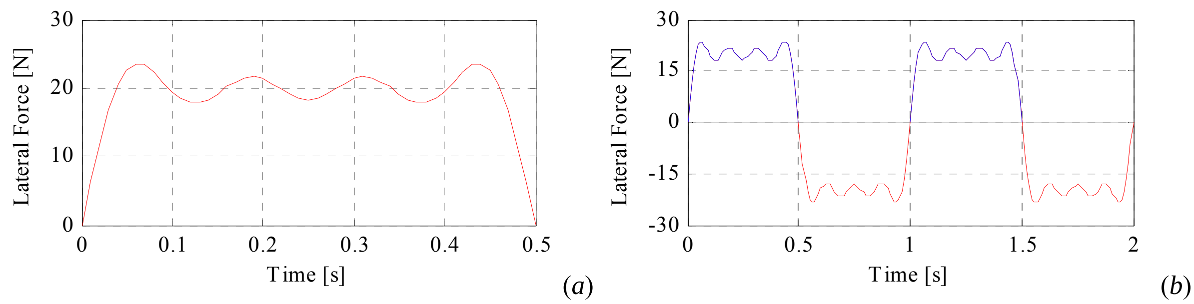

Figure 7: One step (*a*) and periodic walking (*b*) time histories in transverse direction

	Pedestrian Velocity $[m/s^2]$	Vertical Frequency Range [Hz]	Horizontal Frequency Range [Hz]	$\alpha_{1,v}$ [-]	$\alpha_{1,h}$ [-]
Walking	1.3÷ 2.2	1.4 ÷ 2.4	0.7 ÷ 1.2	0.185÷ 0.560	~0.039
Running	1.8÷ 2.9	2.0 ÷ 3.2	1.0 ÷ 1.6	0.431÷ 0.560	~0.039
Jumping	1.3÷3.0	1.4 ÷ 3.4	0.7 ÷ 1.7	0.185÷0.560	~0.039

Table 2: Typical vertical forcing frequencies and velocities due to pedestrian and dynamic load factors

	Vertical Force		Horizontal Force	
Harmonic	$\alpha_{n,v}$	$\varphi_{n,v}$	$\alpha_{n,h}$	$\varphi_{n,h}$
1	$0.41(f_p\text{-}0.95) \leq 0.560$	0°	0.0390	0°
2	0.344	90°	0.0130	0°
3	0.138	90°	0.0078	0°
4	-	-	0.0056	0°

Table 3: Numerical coefficients of pedestrian-induced forces

4.2 Results of dynamic analyses

Several numerical analyses are performed increasing the pedestrian velocity and simulating one or more pedestrians crossing the footbridge. Some relevant results are described in the following and shown in Figures 8, 9. In Figure 8, examples of footbridge accelerations and displacements caused by two people running are reported. The pacing frequency adopted is 3 Hz. The blue and the red lines are referred to nodes positioned in a side span and in the central span, respectively. Values of displacements are small (less than 1 mm); vertical accelerations agree with those measured experimentally (about 30-40 mg), whereas some differences are obtained for lateral accelerations: maximum values of about 8-10 mg are reached while greater values are measured experimentally (about 30 mg, see Figure 3*b*). It is worth noting that these values strongly depend on the imposed numerical damping ratio; thus, the experimental identification of damping ratios must be accurate as well as possible to obtain a reliable comparison between experimental and numerical results.

Finally, in Figure 9 the dynamic amplification factors in terms of accelerations and displacements considering a pedestrian crossing the footbridge with velocity in the range 1.5÷4.5 m/s are reported. The corresponding pacing frequency is also given. Solid and dashed lines represent horizontal and vertical components respectively; moreover, letters A, B and C refer to three nodes placed at midspan and at a quarter of the central span (node A and B) and at midspan of a side span (node C). Significant lateral amplifications are observed for a pacing frequency of about 3.33 Hz, corresponding to a horizontal frequency of 1.665 Hz (i.e. close to the first structural lateral frequency). Vertical amplifications are obtained for a pacing frequency of about 4.15 Hz, quite close to the first vertical frequency of the structure.

5 CONCLUSIONS

In this paper the dynamic behaviour of the Correggio footbridge is investigated, particularly concerning the dynamic amplifications of the structure induced by pedestrian dynamic actions. First, dynamic tests have been performed. Starting from the measured data, the modal properties of the structure are identified applying the EFDD method and the maximum accelerations induced by pedestrian loads are evaluated. Results show a first lateral frequency of 1.67 Hz and a fist vertical frequency of 4.39 Hz. Then, a FE model is built and calibrated, obtaining numerical dynamic properties matching very well the experimental ones. After the model updating, dynamic analyses are performed adopting a single step load model to simu-

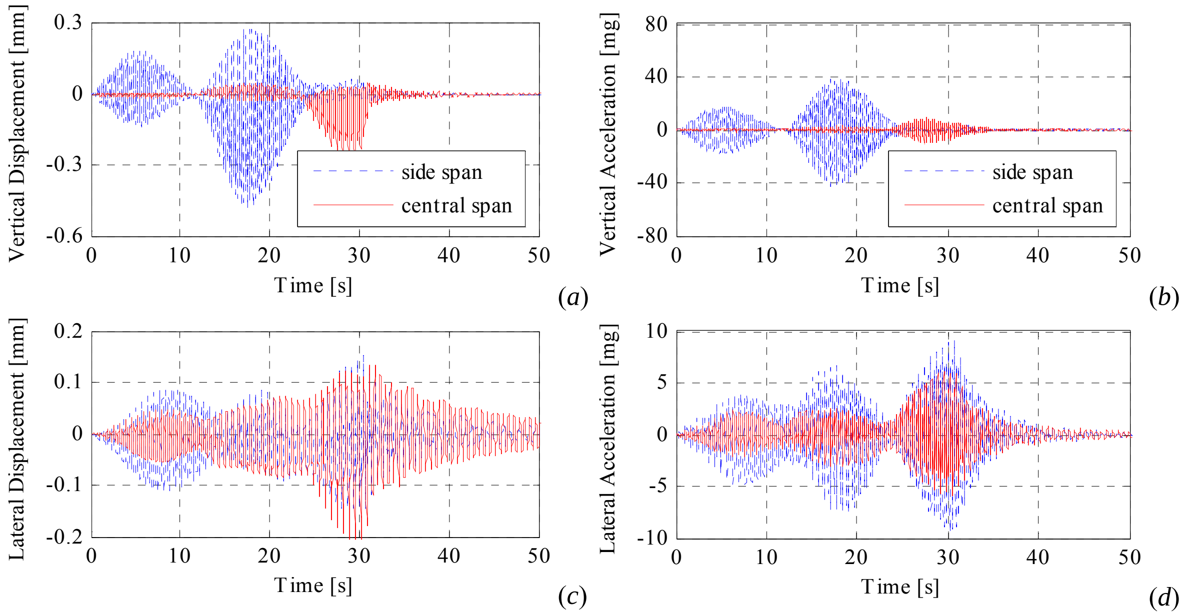

Figure 8: Numerical results: vertical and lateral displacements (*a*,*c*) and accelerations (*b*,*d*) due to running

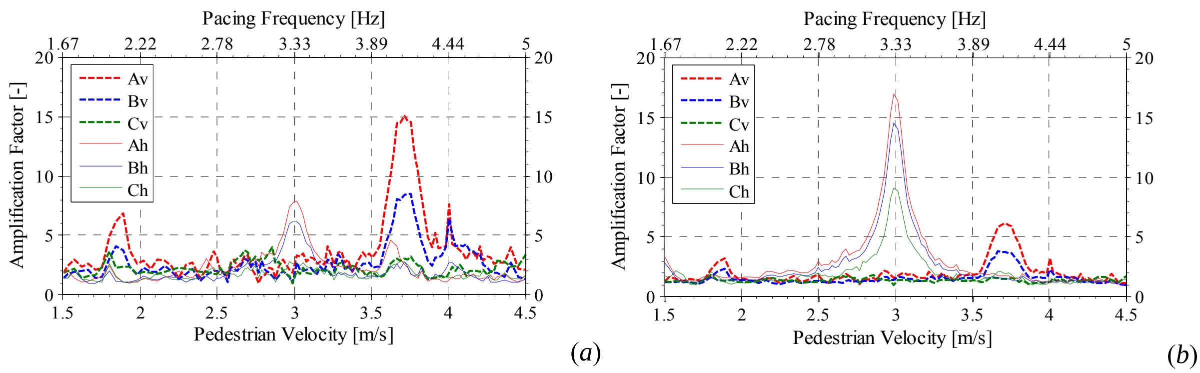

Figure 9: Numerical results: amplification factor in terms of accelerations (*a*) and displacements (*b*) for node A, B and C

late vertical and horizontal pedestrian actions. Finally, numerical and experimental results are compared. Numerical vertical accelerations correspond to experimental ones reaching values of about 30-40 mg, whereas numerical horizontal accelerations are lower. As expected, high dynamic amplifications are obtained for pacing frequencies close to the first lateral and the first vertical frequencies of the structure. The maximum horizontal amplification is achieved at a pedestrian velocity of 3 m/s (fast running), which substantially corresponds to the upper bound of the pedestrian speed range.

ACKNOWLEDGMENTS

Dynamic tests have been performed by using the Teleco SHM602 system. The authors would like to thank V. Simioli and T. Baravelli for the technical support and Teleco S.p.a. for the dynamic equipment.

REFERENCES

[1] P. Dallard, T. Fitzpatrick, A. Flint, S. Le Boutva, A. Low, R. Ridsdill Smith and M. Willford, The London Millennium Footbridge. *The Structural Engineer*, **79**, 17-33, 2001.

[2] F. Danbon and F. Grillaud, Dynamic behaviour of a steel footbridge. Characterization and modeling of the dynamic loading induced by a moving crowd on the Solferino footbridge in Paris. *Proceedings of Footbridge 2005*, Venice, Italy, 2005.

[3] R. Guidorzi, R. Diversi, L. Vincenzi, C. Mazzotti and V. Simioli, Structural monitoring of the Tower of the Faculty of Engineering in Bologna, using MEMS-based sensing. *Proceedings of EuroDyn*, Leuven, Belgium, 2499-2506, 2011.

[4] J. S. Bedant and A. G. Piersol, *Engineering application of correlation and spectral analysis*. John Wiley & Sons, New York, 1986.

[5] R. Brincker, C. Ventura and P. Andersen, Damping estimation by Frequency Domain Decomposition. *Proceedings of the 19th International Modal Analysis Conference*, Kissimmee, USA, 1-6, 2001.

[6] D.J. Ewins, *Modal testing: theory and practice.* John Wiley & Sons, New York, 1986.

[7] Y. Matsumoto, T. Nishioka, H. Shiojiri and K. Matsuzaki, Dynamic design of footbridges. *Proceedings of IABSE Conference*, 1-15, 1978.

[8] P. Young, Improved floor vibration prediction methodologies. *Proceedings of ARUP Vibration Seminar*, Institute of Mechanical Engineers, London, UK, 2001

[9] H. Bachmann, Lively footbridges - a real challenge. *Proceedings of the International Conference on the Design and Dynamic Behaviours of Footbridges*, Paris, France, 1-8, 2002.

[10] S. Zivanovic, A. Pavic and P. Reynolds, Vibration serviceability of footbridges under human-induced excitation: a literature review. *Journal of Sound and Vibration*, **279**, 1-74, 2005.

[11] S.I. Nakamura, Model for lateral excitation of footbridges by synchronous walking. *ASCE Journal of Structural Engineering*, **130**, 32–37, 2004.

[12] British Standards Institution. *Appendix C: vibration serviceability requirements for foot and cycle track bridges.* BSI, London, 1978, BS 5400, Part 2.